PHYSICAL REVIEW B **84**, 180407(R) (2011)

Kitaev-Heisenberg-J_2-J_3 model for the iridates A_2IrO_3

Itamar Kimchi[1] and Yi-Zhuang You[1,2]
[1]*Department of Physics, University of California, Berkeley, California 94720, USA*
[2]*Institute for Advanced Study, Tsinghua University, Beijing 100084, China*
(Received 30 August 2011; revised manuscript received 7 October 2011; published 10 November 2011)

A Kitaev-Heisenberg-J_2-J_3 model is proposed to describe the Mott-insulating layered iridates A_2IrO_3 (A = Na, Li). The model is a combination of the Kitaev honeycomb model and the Heisenberg model with all three nearest-neighbor couplings J_1, J_2, and J_3. A rich phase diagram is obtained at the classical level, including the experimentally suggested zigzag ordered phase; as well as the stripy phase, which extends from the Kitaev-Heisenberg limit to the J_1-J_2-J_3 one. Combining the experimentally observed spin order with the optimal fitting to the uniform magnetic susceptibility data gives an estimate of possible parameter values, which in turn reaffirms the necessity of including both the Kitaev and farther neighbor couplings.

DOI: 10.1103/PhysRevB.84.180407 PACS number(s): 75.10.Jm, 71.27.+a

Frustrated spin systems have long served as a relatively simple yet rich source of exotic phenomena such as spin liquids and unconventional order. The frustration may arise either geometrically on a lattice incompatible with the spin ordering, or dynamically from noncommuting competing terms in the Hamiltonian. The nearest-neighbor $S = 1/2$ Heisenberg model on the kagome lattice is an instance of geometrical frustration that may even host a quantum spin liquid ground state.[1] Bipartite lattices such as the honeycomb can still be geometrically frustrated by including farther than nearest-neighbor antiferromagnetic Heisenberg exchange, giving so-called J_1-J_2-J_3 models. Such models on the honeycomb in particular have seen a recent surge of work,[2–6] though a quantum spin liquid phase may require charge as well as spin fluctuations.[7–9] Breaking spin rotational symmetry provides avenues for dynamical frustration, as in the Kitaev honeycomb model,[10] a nearest-neighbor Ising coupling of a spin component set by a bond label γ as in Fig. 1. This seemingly artificial model is exactly solvable with a spin liquid ground state exhibiting an emergent Majorana fermion with a Z_2 gauge background.

A recent and surprising addition to the experimentally relevant J_1-J_2-J_3 models of frustrated spin systems, the Kitaev coupling, has been recently proposed[11,12] to occur in the Mott-insulating[13] iridates A_2IrO_3 (A = Na, Li), where the iridium ions are arranged in layers of two dimensional honeycomb lattices. Uniform susceptibility and heat capacity studies on these materials[13,14] found Curie-Weiss temperatures of -125 K for Na_2IrO_3 and -33 K for Li_2IrO_3, and a low magnetic ordering temperature of 15 K for both, suggesting strong frustration. A resonant x-ray scattering measurement[15] on Na_2IrO_3 found the ground state has antiferromagnetic order at wave vector M, suggested by a first-principles calculation[15] to be a zigzag rather than a stripy configuration (see Fig. 2).

Strong spin-orbit coupling splits the iridium t_{2g} states into a filled manifold and a half-filled Kramer's doublet, an effective spin-1/2 degree of freedom which need no longer respect the rotational symmetry. Thus the 90° angles of the Ir-O-Ir hopping path within the oxygen octahedra, together with d-orbital Hund's rule coupling and orbital interactions, are able to give the Kramer's doublet highly anisotropic exchanges of the Kitaev form. Higher-order hopping paths, direct orbital overlaps, trigonal distortions, and spin-orbit energy splittings within the iridium two-electron propagator all contribute spin interactions other than the Kitaev term, primarily including antiferromagnetic Heisenberg exchange.

Keeping only the nearest-neighbor Heisenberg exchange yields the Heisenberg-Kitaev model,[12,16–18] Eq. (1), with J_2, J_3 set to zero, which has been previously used to describe the A_2IrO_3 materials.[12–15] The phase diagram[12,16] in the parameter $0 \leqslant \alpha \leqslant 1$ consists of a Néel phase for the Heisenberg model at small $0 \leqslant \alpha < 0.4$, the Kitaev spin liquid at large $0.8 < \alpha \leqslant 1$, and an intermediate antiferromagnetically ordered stripy phase (see Fig. 2). The stripy configuration is the exact ground state at $\alpha = 0.5$, solvable by means of a periodic site-dependent spin rotation[12] which turns the Hamiltonian into a Heisenberg ferromagnet in the rotated spins.

Preserving J_2 and J_3 to produce the previously unstudied Kitaev-Heisenberg-J_2-J_3 model is important for two reasons. First, substantial J_2 and J_3 are likely to exist in the materials; density functional theory (DFT) calculations[19] for Na_2IrO_3 found $J_2/J_1 \approx 0.5$, and a later tight-binding fit of the DFT data including J_3 found J_2, J_3 to be approximately equal.[20] Second, the experimentally suggested zigzag ordered ground state[15] cannot be realized in a Kitaev-Heisenberg model alone. It is found that an antiferromagnetic J_3 term is needed to stabilize the zigzag order. Moderate Kitaev and J_2 couplings stabilize both zigzag and stripy orders. We will also show that in order to reproduce the experimentally measured uniform susceptibility $\chi(T)$, the farther neighbor J_2 and J_3 couplings as well as the Kitaev term are likely needed.

The Kitaev-Heisenberg-J_2-J_3 Hamiltonian is

$$H = J\left[(1-\alpha)\left(\sum_{\langle ij\rangle} + J_2\sum_{\langle\langle ij\rangle\rangle} + J_3\sum_{\langle\langle\langle ij\rangle\rangle\rangle}\right)\boldsymbol{\sigma}_i\cdot\boldsymbol{\sigma}_j - 2\alpha\sum_{\langle ij\rangle}\sigma_i^{\gamma_{ij}}\sigma_j^{\gamma_{ij}}\right], \quad (1)$$

where $\langle ij\rangle$, $\langle\langle ij\rangle\rangle$, and $\langle\langle\langle ij\rangle\rangle\rangle$ stand for the first, second, and third nearest-neighbor bonds, and γ_{ij} is a nearest-neighbor bond label, as illustrated in Fig. 1. The model interpolates between the J_1-J_2-J_3 model at $\alpha = 0$ and the Kitaev model

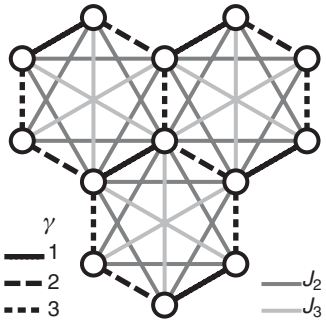

FIG. 1. The honeycomb lattice, with the Kitaev label γ for nearest-neighbor bonds, and including second and third neighbor bonds with Heisenberg couplings J_2 and J_3.

at $\alpha = 1$, maintaining the second and third neighbor coupling strengths J_2 and J_3 in units of the nearest-neighbor Heisenberg coupling strength.

A recently proposed alternative model for Na_2IrO_3 based on *ab initio* calculations[19] takes the limit where trigonal distortion effects are stronger than spin-orbit coupling, finding a Hamiltonian with Ising anisotropy and no Kitaev term.[20,21] Putting this interesting scenario aside,[22] we find that mild $\hat{c} \equiv (1,1,1)$ uniaxial trigonal distortion is consistent with our approach. The effective spin-1/2 Kramer's doublet remains well separated from the filled states. Its modified wave function creates anisotropies in the magnetic field coupling (g-factor tensor) and combines with the non-90° Ir-O-Ir hopping path to perturb Eq. (1), possibly enhancing both Kitaev and Heisenberg terms in addition to creating small Ising $S^{\hat{c}}S^{\hat{c}}$ and Ising-Kitaev $S^{\gamma_{ij}}S^{\hat{c}}$ terms. Both modifications are expected from the observed anisotropy in single-crystal Na_2IrO_3 susceptibility[13] and do not change our results.

Since there is ample evidence[13–15] for magnetic ordering in both Na_2IrO_3 and Li_2IrO_3, we will leave the calculation of the quantum phase diagram of Eq. (1) for future work, instead turning to the magnetically ordered phases which may be studied by a purely classical analysis. For each point (α, J_2, J_3) in the three-dimensional phase diagram we determined the magnetic ordering configurations using a quadratic (unconstrained) classical spin model,[23] which we diagonalized analytically in momentum space. Since $\Gamma = -\Gamma$ and $M = -M$ these two wave vectors automatically give configurations of collinear unit-length normalized spins, despite the absence of the unit-length constraint in the calculation, reaffirming the validity of the classical solution at these points. Solutions at wave vector K or at generic incommensurate wave vectors correspond to noncollinear spiral configurations, which we label as a single phase.

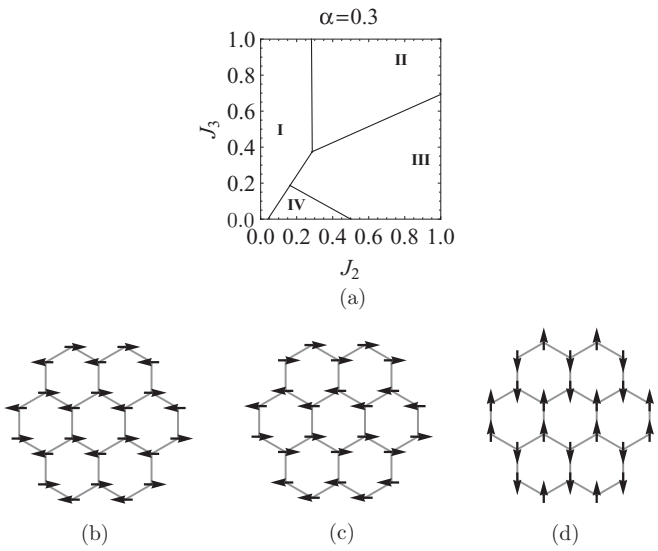

FIG. 2. (a) Sample (J_2, J_3) slice of the classical phase diagram, with phases (I), (II), and (IV) represented in (b), (c), and (d), respectively. Region (III) contains various noncollinear spiral configurations. (b) (I) Néel. (c) (II) Zigzag. (d) (IV) Stripy.

In order to discuss results on the classical phase diagram, we introduce standard nomenclature from the literature. For each ordering wave vector the phases are labeled by a Roman numeral[2,3] as follows: Γ: (I) Néel; M: (IV) stripy;[12] and (II) zigzag[15] (or columnar[6]). All other wave vectors are (III) spiral. Figure 3 displays six (J_2, J_3) slices of the classical phase diagram at various fixed α.

Quantum fluctuations modify the classical phase diagram in two ways. First, they create regions of quantum phases such as the plaquette valence bond solid or the Kitaev spin liquid; the former has been seen in the J_1-J_2-J_3 model,[2] while the latter appears[12,16] at small J_2, J_3 starting at $\alpha \geqslant 0.8$. Second, they shift the boundaries between the magnetically ordered phases. Quantum fluctuations disfavor the spiral configurations[2,3] in favor of the collinear ordered phases, shrinking region (III); they also favor the Néel state (I) over the other orders.[2,12]

The three-dimensional phase diagram offers insights otherwise unavailable in its various limits. The stripy (IV) region in the J_1-J_2-J_3 model at $\alpha = 0$ is in the same phase as the fluctuation-free exactly solvable point $\alpha = 0.5, J_2 = J_3 = 0$, which may be understood only within the Kitaev-Heisenberg model.[12] As α increases, both the stripy and the zigzag phases grow substantially larger. The dynamic frustration by the Kitaev term and the geometric frustration by the J_2 term have similar effects on the ordered phases, destabilizing Néel in favor of stripy and zigzag.

It is worth reporting the direction of magnetic ordering in the various phases (excepting the special points $\alpha = 0$ and $\alpha = 1/2$). The direction of the collinear magnetic ordering in both stripy and zigzag phases is constrained already at the classical level. For M_z stripy order the spins lie along S^z, as was already determined by the spin rotation[12] solution of the $J_2 = J_3 = 0$, $\alpha = 0.5$ Hamiltonian. For zigzag order we found that the spins are constrained to the S^xS^y plane (see Fig. 2). Thermal and quantum fluctuations ("order from disorder") force the spins to lie along a cubic axis within the classically allowed space, in this case the S^x and S^y axes. Trigonal distortion gives other perturbations: For example, for M_z stripy order it cants the spin axis from S^z toward the distortion axis, and for the Néel phase the distortion axis may be an energy minimum or maximum within the Bloch sphere. A linear spin-wave analysis found that directions closest to cubic axes are still preferred by quantum fluctuations. However, anisotropy in the real material likely overcomes all these effects to determine the ordering direction.[15]

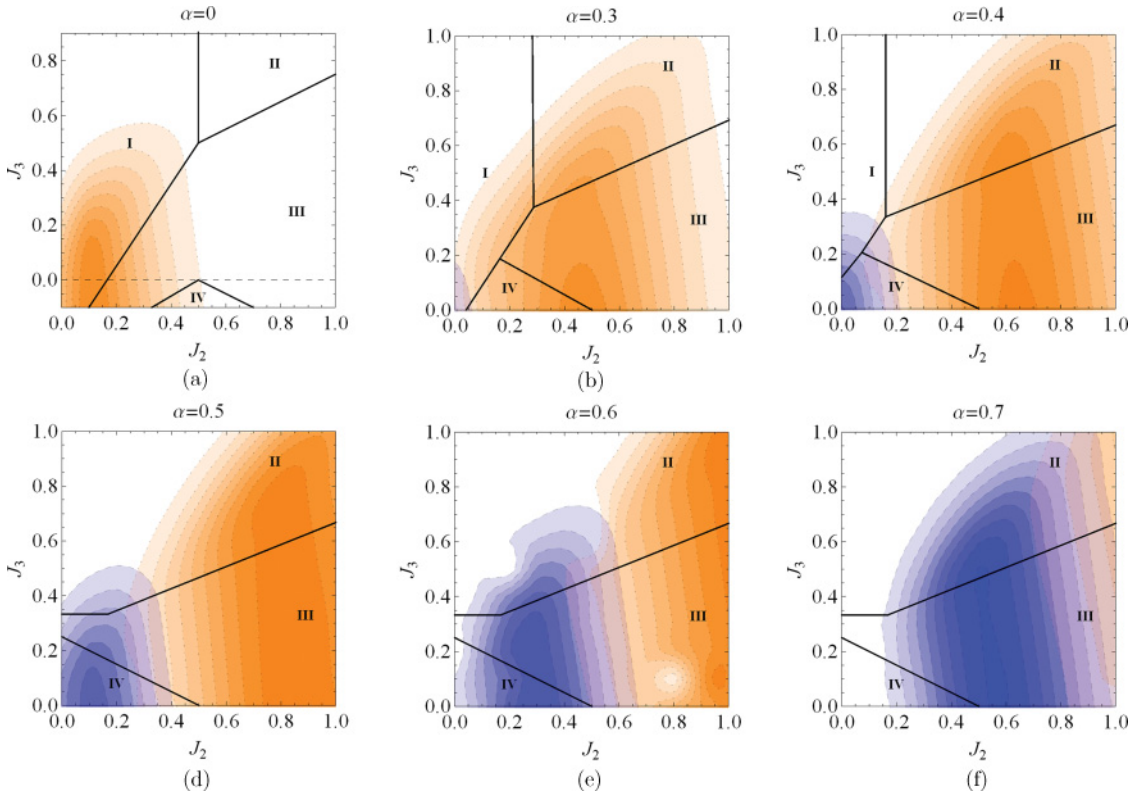

FIG. 3. (Color online) Fixed α slices in (J_2, J_3) showing the magnetically ordered phases (I,II,III,IV) = Neel, zigzag, spiral, stripy) and shading corresponding to the ED $\chi(T)$ fit goodness. Increasing the Kitaev term (i.e., increasing α) enlarges the extent of the zigzag and stripy phases, which occur at both small and large α. Fits to Na_2IrO_3 are shaded in orange (with dotted contour lines) and fits to Li_2IrO_3 are in blue (with dashed contour lines); darker shading corresponds to good fitting with $\mu/\mu_B \approx 1$ and $J_2 \gtrsim J_3$, while lighter shading corresponds to poor agreement. Given a magnetically ordered ground state for each of the materials, the range of allowed parameters is found by intersecting the darker shaded region with the magnetically ordered phase.

Next we discuss the comparisons between experimentally measured susceptibility[13,14] and exact diagonalization (ED), first describing each in turn. Uniform magnetic susceptibility data for the sodium and lithium materials at temperatures up to 300 K was taken from the most recent study,[14] with the constant background removed.[14] We used data from temperatures above 150 K in order to avoid finite-size effects when comparing to ED. ED using the "fulldiag" ALPS module[24] was performed keeping all eigenstates to enable comparison with high-temperature data. The system diagonalized was an eight-spin cluster, the unit cell of the $\alpha = 1/2$ site dependent spin rotation,[12] with periodic boundary conditions. As expected, the eight-spin ED, corresponding to a high-temperature series expansion with eight-spin clusters, is reliable to far lower temperatures than the two-spin Curie-Weiss expression, which only holds at $T \gg J$.We found that ED finite-size effects for eight-spin clusters were only visible in the susceptibility at low temperatures $T \lesssim J/2$, well below J. The highest J values needed for good fits were below the 150 K data cutoff, self-consistently affirming the reliability of the ED fits.

For each parameter set (α, J_2, J_3) we diagonalized the system to generate a curve $\chi(T)$. The Hamiltonian Eq. (1) with a magnetic field coupling term has two parameters in addition to (α, J_2, J_3), namely, the overall scale J and the magnetic field coupling $g\mu$. Since the effective spin-1/2 turns out to have the same g factor as an electron spin, we fix $g = 2$ and expect μ/μ_B to remain close to $\mu/\mu_B = 1$. For each (α, J_2, J_3) point the curve $\chi(T)$ was fit to the experimental data by the two parameters J (corresponding to horizontal stretching) and μ/μ_B (with $(\mu/\mu_B)^2$ corresponding to vertical stretching). The resulting fit was evaluated by a "goodness function," the product of three Gaussian distributions, enforcing the following three conditions for a good fit. First, the magnetic moment μ/μ_B found by the best fit must be close to 1, with a standard deviation of 0.15. This constraint on μ effectively constrained J as well. Second, the root-mean-square relative fit residual must be near zero with a standard deviation of 10^{-3}. Third, the third neighbor coupling must be smaller or not much larger than the second neighbor coupling $J_3 \lesssim J_2$, relaxed by a standard deviation of 0.2. The absolute (unscaled) value of

TABLE I. Parameters for given M-wave vector order.

		Na_2IrO_3	
Stripy (IV)	$\alpha \approx 0.2$–0.3	$J_2 \lesssim 0.5, J_3 \lesssim 0.2$	$J \approx 110$ K
Zigzag (II)	$\alpha \approx 0.4$–0.6	$J_2, J_3 \gtrsim 0.4$	$J \approx 100$ K
		Li_2IrO_3	
Stripy (IV)	$\alpha \approx 0.5$	$J_2, J_3 \lesssim 0.3$	$J \approx 100$ K
Zigzag (II)	$\alpha \approx 0.7$	$J_2, J_3 \gtrsim 0.4$	$J \approx 90$ K

this goodness function was used to produce the shading in Fig. 3, with darker shading corresponding to better fits.

Given knowledge of the ground-state magnetic order in Na_2IrO_3 and Li_2IrO_3, appropriate values for α, J_2, and J_3 are found by intersecting the darker shaded regions in Fig. 3 with the domain of the ordered phase. The estimated Na_2IrO_3 and Li_2IrO_3 parameters given either stripy or zigzag magnetic order are summarized in Table I. All material and order combinations yielded fitted values of J in the range $J \approx 60$–150 K, with the likeliest values $J \approx 100$ K. The lithium material has less structural distortion than the sodium material,[14] suggesting a larger α, in agreement with the fitting results if they have the same magnetic order. For zigzag ordered Li_2IrO_3 we find $\alpha \approx 0.7$, i.e., $J_K \sim 4$–$5J_1$ with a numerical value of $J_K \approx 130$ K. Such a large Kitaev term relative to the other couplings suggests that the Kitaev spin liquid phase may be within experimental reach.[14] In particular, doping Li_2IrO_3 may suppress its magnetic order to reveal characteristics of a doped Kitaev spin liquid.[25]

In conclusion, we propose the Kitaev-Heisenberg-J_2-J_3 model, determining its ordered phases, and further using ED fits of susceptibility measurements to demonstrate its applicability to Na_2IrO_3 and Li_2IrO_3. We find that the geometrical frustration due to J_2, J_3 and the dynamical frustration due to the Kitaev term both stabilize the same unconventional stripy and zigzag ordered ground states before the onset of the Kitaev spin liquid. We extract appropriate values for the spin couplings by first restricting to the experimentally observed magnetic order in the phase diagram, and then by requiring good fitting of the susceptibility $\chi(T)$ by ED data. For zigzag ordered Li_2IrO_3, a significant Kitaev term $J_K \approx 130$ K, five times larger than the nearest-neighbor Heisenberg coupling, as well as substantial J_2 and J_3 couplings, are required for good agreement with experimental data.

We are grateful to Ashvin Vishwanath, Tarun Grover, and Hong Yao for valuable discussions and to Ashvin Vishwanath and Michael P. Zaletel for thoughtful comments on the manuscript. This work is supported in part by the National Science Foundation under Grant No. DGE 1106400 (I.K.), and by the China Scholarship Council and the Tsinghua Education Foundation in North America (Y.Z.Y.).

[1] S. Yan, D. A. Huse, and S. R. White, Science **332**, 6034 (2011).
[2] A. F. Albuquerque, D. Schwandt, B. Hetényi, S. Capponi, M. Mambrini, and A. M. Läuchli, Phys. Rev. B **84**, 024406 (2011).
[3] J. B. Fouet, P. Sindzingre, and C. Lhuillier, Eur. Phys. J. B **20**, 241 (2001).
[4] J. Reuther, D. A. Abanin, and R. Thomale, Phys. Rev. B **84**, 014417 (2011).
[5] D. J. J. Farnell, R. F. Bishop, P. H. Y. Li, J. Richter, and C. E. Campbell, Phys. Rev. B **84**, 012403 (2011).
[6] J. Oitmaa and R. R. P. Singh, Phys. Rev. B **84**, 094424 (2011).
[7] Z. Y. Meng, T. C. Lang, S. Wessel, F. F. Assaad, and A. Muramatsu, Nature (London) **464**, 847 (2010).
[8] B. K. Clark, D. A. Abanin, and S. L. Sondhi, Phys. Rev. Lett. **107**, 087204 (2011).
[9] H. Y. Yang and K. P. Schmidt, Europhys. Lett. **94**, 17004 (2011).
[10] A. Yu. Kitaev, Ann. Phys. **321**, 2 (2006).
[11] G. Jackeli and G. Khaliullin, Phys. Rev. Lett. **102**, 017205 (2009).
[12] J. Chaloupka, G. Jackeli, and G. Khaliullin, Phys. Rev. Lett. **105**, 027204 (2010).
[13] Y. Singh and P. Gegenwart, Phys. Rev. B **82**, 064412 (2010).
[14] Y. Singh, S. Manni, and P. Gegenwart, e-print arXiv:1106.0429.
[15] X. Liu, T. Berlijn, W.-G. Yin, W. Ku, A. Tsvelik, Young-June Kim, H. Gretarsson, Yogesh Singh, P. Gegenwart, and J. P. Hill, Phys. Rev. B **83**, 220403(R) (2011).
[16] H.-C. Jiang, Z.-C. Gu, X.-L. Qi, and S. Trebst, Phys. Rev. B **83**, 245104 (2011).
[17] J. Reuther, R. Thomale, and S. Trebst, Phys. Rev. B **84**, 100406(R) (2011).
[18] F. Trousselet, G. Khaliullin, and P. Horsch, Phys. Rev. B **84**, 054409 (2011).
[19] H. Jin, H. Kim, H. Jeong, C. H. Kim, and J. Yu, e-print arXiv:0907.0743.
[20] S. Bhattacharjee, S. S. Lee, and Y. B. Kim, e-print arXiv:1108.1806.
[21] For a related result see B. J. Yang and Y. B. Kim, Phys. Rev. B **82**, 085111 (2010).
[22] An alternative scenario is explored in A. Shitade, H. Katsura, J. Kunes, X.-L. Qi, S.-C. Zhang, and N. Nagaosa, Phys. Rev. Lett. **102**, 256403 (2009).
[23] P. W. Anderson, Phys. Rev. **79**, 705 (1950).
[24] ALPS collaboration [http://alps.comp-phys.org/]: B. Bauer *et al.*, J. Stat. Mech. (2011) P05001; A. F. Albuquerque *et al.*, J. Magn. Magn. Mater. **310**, 1187 (2007).
[25] Yi-Zhuang You, Itamar Kimchi, and Ashvin Vishwanath, e-print arXiv:1109.4155.